Journal of Physics: Conference Series

Optimal Control of the Wilcox turbulence model with lifting functions for flow injection and boundary control

IOP Conf. Series: Journal of Physics: Conf. Series **1224** (2019) 012006 doi:10.1088/1742-6596/1224/1/012006

Optimal Control of the Wilcox turbulence model with lifting functions for flow injection and boundary control

L Chirco[1], A Chierici[1], R Da Vià[1], V Giovacchini[1] and S Manservisi[1]

[1] Department of Industrial Engineering DIN
Laboratory of Montecuccolino
University of Bologna
Via dei Colli 16, Bologna 40136 (BO), Italy

E-mail: leonardo.chirco2@unibo.it

Abstract. This paper deals with boundary optimal control problems for the Navier-Stokes equations and Wilcox turbulence model. In this paper we study adjoint optimal control problems for Navier-Stokes equations to improve the advantages of using simulations where turbulence models play a significant role in designing engineering devices. We assess first distributed optimal control problems with the purpose to control the fluid behavior by injecting a flow on the boundary solid region to obtain a desired control over the fluid velocity and the kinetic turbulence energy in specific parts of the domain. Then, with the same purpose, we use lifting functions and boundary control. For this reason we reformulate the boundary optimal control problem into a distributed problem through a lifting function approach. The stronger regularity requirements which are imposed by standard boundary control approaches can then be avoided. The state, adjoint and control equations are derived and the optimality system solved for some simple cases with a finite element. Furthermore, we propose numerical strategies that allow to solve the coupled optimality system in a robust way for a large number of unknowns. The approach presented in this work is general and can be used to assess different objectives and types of control.

1. Introduction

In the last several years optimization techniques have gained attention in several research fields of fluid dynamics. Optimal control theory has been applied successfully to many fields ranging from heat transfer problems to fluid-structure interaction systems. Most of the works refers to the standard Navier-Stokes system [1, 2]. However, if a turbulence problem is considered then a direct simulation of the Navier-Stokes system is unpractical due to the computational effort required. In this work we consider the Reynolds averaged Navier-Stokes (RANS) system for the computation of the average pressure and velocity fields. The closure of the problem is guaranteed by the implementation of the Wilcox $k-\omega$ model. Its accuracy and stability allow the coupling between turbulence and the theory of optimal control. In particular, if appropriate limits are taken into account the $k-\omega$ model has regular solutions over large range of parameters [3].

Distributed control strategies, feedback control and adjoint mehods, have been successfully achieved in previous works both for DNS and RANS system while the implementation of a boundary control is not a trivial task [4, 5, 6]. The main difficulty concerns the mathematical

definition of the boundary control parameters. Boundary functions belong to the trace spaces restriction of the natural state volume spaces. It would be necessary to introduce a fractional norm to express the penalization of the cost functional associated to the control parameter. Due to the difficulty of this task usually stronger regularity requirements are imposed. This process leads to controls smoother than necessary due to over-penalization that can affect the accuracy of the solution. For this reasons in this work we aim to achieve a boundary control of the RANS system through a lifting function approach which consists of reformulation of the boundary control problem into a distributed one. By introducing the lifting function approach boundary controls are defined in the appropriate function boundary spaces restriction of the natural state volume spaces [7, 8].

In the present work we introduce an alternative formulation of the lifting function approach, where a distributed parameter $\mathbf{f}$ is defined over an external auxiliary domain that includes the controlled boundary. The optimal boundary control is then obtained by restricting the state solution corresponding to the optimal distributed control. In this way, we can express the cost functional by using standard norms on volume spaces. Furthermore, the information obtained with the distributed control can be used to design blowing or suction on the fluid from the boundary. The method presented here can replace a traditional optimization process based on a parametric analysis of the blowing section velocity profile. We use the adjoint method based on the Lagrange multipliers method [9]. The optimality system for the RANS equations closed with the $k-\omega$ turbulence model is derived. We consider two objectives. The first one is a velocity profile matching problem and the second one a turbulence enhancement case. Once that the type of control and the objective are chosen, the complete Lagrangian can be written considering the RANS system and the $k-\omega$ Wilcox model as constraints in order to derive the so-called optimality system. The numerical solution of the optimality system is then performed through a standard Galerkin method implemented in an in-house finite element C++ code with a steepest descent algorithm for the search of the local minimum of the functional.

2. Mathematical model

In this section we introduce the mathematical model describing our optimal control problem. We first report the conservation equations modeling the physical system and then define the objective functional through which we achieve the optimality system.

We use standard notation $H^s(\Omega)$ for the Sobolev spaces of square integrable functions with square integrable weak derivatives up to order s. We denote with $\langle\cdot,\cdot\rangle_s$ the scalar product in $H^s(\Omega)$ and the induced norm is $||\cdot||_m = \sqrt{(\cdot,\cdot)_m}$. Let $H_0^s(\Omega)$ be the space of all functions in $H^s(\Omega)$ that vanish of the boundary of the bounded open set Ω. We denote with $H^{-s}(\Omega)$ the dual space of $H_0^s(\Omega)$. The trace space for the functions in $H^1(\Omega)$ is denoted by $H^{1/2}(\Gamma)$ and its dual by $H^{-1/2}(\Gamma)$. Given any subset $\Gamma_s \subset \Gamma$, we denote by $H^1_{\Gamma_s}(\Omega)$ the subspace of $H^1(\Omega)$ containing functions with vanishing trace on Γ_s, i.e.

$$H^1_{\Gamma_s}(\Omega) = \Big\{ u \in H^1(\Omega) | \gamma_{\Gamma_s} u = 0 \Big\}, \tag{1}$$

where we use the trace restriction operator on Γ_s denoted with γ_{Γ_s} [10]. At last, we define the space of square integrable functions having zero mean over Ω as

$$L^2_0(\Omega) = \Big\{ p \in L^2(\Omega) | \int_\Omega p \; dx = 0 \Big\}. \tag{2}$$

2.1. Conservation equations

In this work we consider the Reynolds averaged Navier-Stokes system for the computation of the average velocity and pressure fields $(\mathbf{u}, p)$ coupled with Wilcox $k-\omega$ turbulence model. The

RANS system consists in the averaged conservation equation of mass and momentum for a fluid. We use Boussinesq's assumption to define the Reynolds' stress tensor introducing the turbulent or eddy viscosity ν_t

$$\boldsymbol{\nabla} \cdot \mathbf{u} = 0 \ , \tag{3}$$

$$(\mathbf{u} \cdot \boldsymbol{\nabla})\mathbf{u} \ = -\boldsymbol{\nabla} p + \boldsymbol{\nabla} \cdot [(\nu + \nu_t)\mathbf{S}(\mathbf{u})] + \mathbf{f} \ , \tag{4}$$

where $\mathbf{f}$ is a force acting on the flow. The closure is obtained by modeling the eddy viscosity through two differential equation for the turbulent kinetic energy k and its specific dissipation rate ω

$$(\mathbf{u} \cdot \boldsymbol{\nabla})k = \boldsymbol{\nabla} \cdot [(\nu + \sigma_k \nu_t)\boldsymbol{\nabla} k] + P_k - \beta^* k\omega \ , \tag{5}$$

$$(\mathbf{u} \cdot \boldsymbol{\nabla})\omega = \boldsymbol{\nabla} \cdot [(\nu + \sigma_\omega \nu_t)\boldsymbol{\nabla} \omega] + \alpha \frac{\omega}{k} P_k - \beta \omega^2 + \frac{\sigma_d}{\omega} \boldsymbol{\nabla} k \cdot \boldsymbol{\nabla} \omega \ , \tag{6}$$

where $\mathbf{S}(\mathbf{u})$ is the deformation tensor and P_k is the production term of the turbulent kinetic energy

$$\mathbf{S}(\mathbf{u}) = \boldsymbol{\nabla}\mathbf{u} + \boldsymbol{\nabla}\mathbf{u}^T \qquad\qquad P_k = \frac{\nu_t}{2} \mathbf{S}(\mathbf{u}) : \mathbf{S}(\mathbf{u}) \ . \tag{7}$$

Furthermore, for the eddy viscosity ν_t of the turbulence model we assume

$$\nu_t = \min\Big[\frac{k}{\omega}, \nu_{max}\Big] \ . \tag{8}$$

The system (3-6) is completed with the appropriate boundary conditions reported in Table 1, where we denoted with Γ_i, Γ_w and Γ_o the fluid inlet, walls and outlet, respectively. We use a near-wall approach [11] for the solution of the turbulence problem, so the RANS equations are integrated throughout the viscous layer. We set the boundary conditions in the linear region at a distance y_d from the wall, so that the value of ω remains limited in the computational domain.

Variable	Γ_i	Γ_w	Γ_o
$\mathbf{u} \cdot \widehat{\mathbf{n}}$	$\mathbf{u}_i$	0	$\boldsymbol{\tau} \cdot \widehat{\mathbf{n}} = 0$
$\mathbf{u} \cdot \widehat{\mathbf{t}}$	0	$\boldsymbol{\tau} \cdot \widehat{\mathbf{n}} = \dfrac{\nu \mathbf{u} \cdot \widehat{\mathbf{t}}}{y_d}$	$-$
P	$-$	$-$	0
k	$k = k_i$	$\boldsymbol{\nabla} k \cdot \widehat{\mathbf{n}} = \dfrac{2k}{y_d}$	$\boldsymbol{\nabla} k \cdot \widehat{\mathbf{n}} = 0$
ω	$\omega = \omega_i$	$\omega = \dfrac{2\nu}{\beta^* y_d^2}$	$\boldsymbol{\nabla} \omega \cdot \widehat{\mathbf{n}} = 0$

Table 1. State variables boundary conditions with near wall approach.

2.2. Boundary optimal control and lifting function

Let Γ_c be a subset of the boundary Γ of the domain $\Omega \subset \mathbb{R}^3$. The first step to obtain the optimality system is to choose an objective for our optimal control problem. The objective functional is denoted by $\mathcal{F}(\mathbf{u}, k)$ and is described by the following expression

$$\mathcal{F}(\mathbf{u}, k, \mathbf{f}) = \frac{a}{2} \int_\Omega ||\mathbf{u} - \mathbf{u}_d||^2 \ d\Omega + \frac{b}{2} \int_\Omega |k - k_d|^2 \ d\Omega \ , \tag{9}$$

where a and b are weight functions. If $b = 0$ we have a velocity matching problem and the objective is expressed as the distance in norm of the velocity from a target value $\mathbf{u}_d$. Similarly, if $a = 0$ the objective concerns the turbulent kinetic energy and its distance from the target k_d. We introduce the boundary condition

$$\mathbf{u} = \mathbf{g} \quad on\ \Gamma_c\,, \tag{10}$$

where $\mathbf{g} \in H^{1/2}(\Gamma_c)$ is the boundary control parameter. In standard boundary control approaches the objective functional is reformulated as

$$\mathcal{J}_b(\mathbf{u}, k, \mathbf{g}) = \frac{a}{2}\int_\Omega ||\mathbf{u} - \mathbf{u}_d||^2\ d\Omega + \frac{b}{2}\int_\Omega |k - k_d|^2\ d\Omega + \frac{\beta}{2}\int_{\Gamma_c} ||\mathbf{g}||^2\ d\Gamma + \frac{\gamma}{2}\int_{\Gamma_c} ||\boldsymbol{\nabla}\mathbf{g}||^2\ d\Gamma\ . \tag{11}$$

The last two terms are penalty regularization contributions introduced to limit the norm of the boundary control function $\mathbf{g}$ and of its gradient. However, by doing so some boundary control solutions becomes unacceptable. We then choose to determine an optimal distributed control from which any and all possible boundary controls can be determined by trace restriction. The cost functional changes so that the penalization terms involves the distributed control. To this end, we define the decomposition of the velocity field given by

$$\mathbf{u} = \mathbf{w} + \mathbf{u}' \quad \text{on } \Omega\ , \tag{12}$$

so that

$$\gamma_{\Gamma_c}\mathbf{u}' = \mathbf{g}\ , \quad \gamma_{\Gamma_c}\mathbf{w} = \mathbf{0}\ . \tag{13}$$

The functions $\mathbf{u}'$ is called lifting function and is the new control parameter, while the velocity $\mathbf{w}$ is the new state variable. Both of them are divergence-free fields

$$\boldsymbol{\nabla}\cdot\mathbf{u}' = 0\ , \quad \boldsymbol{\nabla}\cdot\mathbf{w} = 0 \quad \text{on } \Omega\ . \tag{14}$$

The velocity on Γ_c is determined by trace restriction of lifting function $\mathbf{u}'$ on that boundary, in this way $\mathbf{g} \in H^{1/2}(\Gamma_c)$, the natural space of definition. By substitution it is obtained the following form of state equation of Navier-Stokes

$$\mathbf{w}\cdot\boldsymbol{\nabla}\mathbf{w}\ + \boldsymbol{\nabla}p - \boldsymbol{\nabla}\cdot[(\nu+\nu_t)\mathbf{S}(\mathbf{w})]\ = \mathbf{f}(\mathbf{u}', \mathbf{w})\ , \tag{15}$$

where we have a force term depending on the lifting function and state velocity. We define the cost functional

$$\mathcal{J}(\mathbf{w}, \mathbf{u}') = \frac{a}{2}\int_\Omega ||\mathbf{w}+\mathbf{u}'-\mathbf{u}_d||^2\ d\Omega + \frac{b}{2}\int_\Omega |k-k_d|^2\ d\Omega + \frac{\beta}{2}\int_\Omega ||\mathbf{u}'||^2\ d\Omega + \frac{\gamma}{2}\int_\Omega ||\boldsymbol{\nabla}\mathbf{u}'||^2\ d\Omega\ . \tag{16}$$

We remark the difference between the regularization terms appearing in (11) and (16). The former involves the $H^1(\Gamma)$ norm whereas the latter involves the $H^1(\Omega)$ norm [12].

We now present a new lifting function strategy. Let Ω_{aux} be an extension of the domain Ω sharing with it the boundary Γ_c. We consider the Navier-Stokes equation for the velocity field $\mathbf{u} \in H^1(\Omega)$ without distributed forces

$$\begin{aligned} \mathbf{u}\cdot\boldsymbol{\nabla}\mathbf{u}\ + \boldsymbol{\nabla}p - \boldsymbol{\nabla}\cdot[(\nu+\nu_t)\mathbf{S}(\mathbf{u})]\ &= \mathbf{0} \quad \text{on } \Omega\ , \\ \mathbf{u} &= \mathbf{g} \quad \text{on } \Gamma_c\ . \end{aligned} \tag{17}$$

We define the lifting function on the auxiliary domain $\mathbf{u}' \in H^1(\Omega_{aux})$ so that $\mathbf{u}' = \mathbf{g}$ on Γ_c. It is then possible to formulate a Navier-Stokes equation also for the velocity field $\mathbf{u}'$ on the domain Ω_{aux}

$$\begin{aligned} \mathbf{u}'\cdot\boldsymbol{\nabla}\mathbf{u}'\ + \boldsymbol{\nabla}p - \boldsymbol{\nabla}\cdot[(\nu+\nu_t)\mathbf{S}(\mathbf{u}')]\ &= \mathbf{f} \quad \text{on } \Omega_{aux}\ , \\ \mathbf{u}' &= \mathbf{g} \quad \text{on } \Gamma_c\ . \end{aligned} \tag{18}$$

The force term $\mathbf{f}$ appears only in the right-hand-side of this equation since we can model the velocity in the auxiliary domain as we wish, as long as the boundary condition on Γ_c is respected. Due to this boundary condition there has to be continuity between the solutions of problem (17) and (18) so that we can write

$$\mathbf{u}\cdot\boldsymbol{\nabla}\mathbf{u} \ + \boldsymbol{\nabla}p - \boldsymbol{\nabla}\cdot[(\nu+\nu_t)\mathbf{S}(\mathbf{u})] \ = \ \mathbf{f} \quad \text{on } \Omega\cup\Omega_{aux} \ . \tag{19}$$

Since the optimal distributed control $\mathbf{f}$ acts only on Ω_{aux} then the cost functional becomes

$$\mathcal{J}(\mathbf{u},\mathbf{f}) = \frac{a}{2}\int_\Omega ||\mathbf{u}-\mathbf{u}_d||^2 \ d\Omega + \frac{b}{2}\int_\Omega |k-k_d|^2 \ d\Omega + \frac{\lambda}{2}\int_{\Omega_{aux}} ||\mathbf{f}||^2 \ d\Omega \ . \tag{20}$$

The last term represents the cost of the regularization of the control parameter $\mathbf{f}$ constraining $\mathbf{f} \in L^2(\Omega)$. The amount of regularization is controlled by the positive parameter λ, called regularization parameter and its value plays a key role in the solution of the control problem. If $\lambda = 1$ we have that $\mathbf{f}$ is a square integrable function but the control can be not effective. If $\lambda \to 0$ the control becomes irregular and this lack of regularization leads to convergence issues.

2.3. Optimality system

To obtain the optimality system we write the total Lagrangian of the optimal control problem, by considering the objective functional (20) and the constraints system (3-6). In order to include (8) in the Lagrangian we add the constraint

$$\Big(\nu_t - \frac{k}{\omega}\Big)(\nu_t - \nu_{max}) = 0 \ , \tag{21}$$

and introduce two new real variables γ_1 and γ_2 defined as

$$\gamma_1^2 = \nu_{max} - \nu_t \ , \qquad \gamma_2^2 = \frac{k}{\omega} - \nu_t \ . \tag{22}$$

The unknown state is defined by $(\mathbf{u}, p, \nu_t, k, \omega, \gamma_1, \gamma_2)$. The total Lagrangian is then given by

$$\begin{aligned}
&\mathcal{L}(\mathbf{u},\mathbf{u}_a,p,p_a,k,k_a,\omega,\omega_a,\nu_t,\nu_a,\gamma_1,\gamma_{a1},\gamma_2,\gamma_{a2},\mathbf{f}) = \mathcal{J}(\mathbf{u},k,\mathbf{f}) + \int_\Omega p_a\boldsymbol{\nabla}\cdot\mathbf{u} \ d\Omega + \\
&+ \int_\Omega \mathbf{u}_a\cdot\{(\mathbf{u}\cdot\boldsymbol{\nabla})\mathbf{u} \ + \boldsymbol{\nabla}p - \boldsymbol{\nabla}\cdot[(\nu+\nu_t)\mathbf{S}(\mathbf{u})] \ - \mathbf{f}\} \ d\Omega + \\
&+ \int_\Omega k_a\{\mathbf{u}\cdot\boldsymbol{\nabla}k - \boldsymbol{\nabla}\cdot\Big[\Big(\nu+\frac{\nu_t}{\sigma_k}\Big)\boldsymbol{\nabla}k\Big] - P_k + \beta^* k\omega\} \ d\Omega + \\
&+ \int_\Omega \omega_a\{\mathbf{u}\cdot\boldsymbol{\nabla}\omega - \boldsymbol{\nabla}\cdot\Big[\Big(\nu+\frac{\nu_t}{\sigma_\omega}\Big)\boldsymbol{\nabla}\omega\Big] - \alpha\frac{\omega}{k}P_k + \beta\omega^2 - \frac{\sigma_d}{\omega}\boldsymbol{\nabla}k\cdot\boldsymbol{\nabla}\omega\} \ d\Omega + \\
&+ \int_\Omega \nu_a\Big(\nu_t - \frac{k}{\omega}\Big)(\nu_t-\nu_{max}) \ d\Omega \ + \ \int_\Omega \gamma_{a1}(\nu_{max}-\nu_t-\gamma_1^2) \ d\Omega + \\
&+ \ \int_\Omega \gamma_{2a}\Big(\frac{k}{\omega} - \nu_t - \gamma_2^2\Big) \ d\Omega \ .
\end{aligned} \tag{23}$$

To obtain the optimality system we impose the minimization conditions $\delta\mathcal{L} = 0$. Since the variations with respect to all the variables involved are independent then each variation has to be zero. In this way we obtain the weak form of the adjoint equations used in a finite element discretization (see more details in [13])

$$\int_\Omega \boldsymbol{\nabla}\cdot\mathbf{u}_a\psi_a \ d\Omega = 0 \ , \quad \psi_a \in L^2(\Omega) \tag{24}$$

$$\int_\Omega \{a(\mathbf{u}-\mathbf{u}_d)\boldsymbol{\phi_a} + p_a\boldsymbol{\nabla}\cdot\boldsymbol{\phi_a} + \mathbf{u}_a\cdot(\boldsymbol{\phi_a}\cdot\boldsymbol{\nabla})\mathbf{u} + \mathbf{u}_a\cdot(\mathbf{u}\cdot\boldsymbol{\nabla})\boldsymbol{\phi_a} + \\ - \mathbf{u}_a\cdot\boldsymbol{\nabla}\cdot[(\nu+\nu_t)\mathbf{S}(\boldsymbol{\phi_a})] + + k_a\boldsymbol{\phi_a}\cdot\boldsymbol{\nabla}k - k_a\nu_t\mathbf{S}(\boldsymbol{\phi_a}):\mathbf{S}(\mathbf{u}) + \\ + \omega_a\boldsymbol{\phi_a}\cdot\boldsymbol{\nabla}\omega - \alpha\omega_a\mathbf{S}(\boldsymbol{\phi_a}):\mathbf{S}(\mathbf{u})\}\, d\Omega = 0\ , \qquad \forall\boldsymbol{\phi_a}\in\mathbf{H}^1_{\Gamma_i,,\Gamma_{o,t},\Gamma_{w,n}}(\Omega) \tag{25}$$

$$\int_\Omega \Big\{b(k-k_d)\varphi_a + k_a\mathbf{u}\cdot\boldsymbol{\nabla}\varphi_a - k_a\boldsymbol{\nabla}\cdot\Big[\Big(\nu+\frac{\nu_t}{\sigma_k}\Big)\boldsymbol{\nabla}\varphi_a\Big] + k_a\beta^*\omega\varphi_a + \\ - \omega_a\frac{\sigma_d}{\omega}\boldsymbol{\nabla}\varphi_a\cdot\boldsymbol{\nabla}\omega + \frac{\gamma_{2a}-\nu_a(\nu_t-\nu_{max})}{\omega}\varphi_a\Big\}d\Omega = 0, \qquad \forall\varphi_a\in H^1_{\Gamma_i}(\Omega) \tag{26}$$

$$\int_\Omega \Big\{k_a\beta^*k\gamma + \omega_a\mathbf{u}\cdot\boldsymbol{\nabla}\gamma - \omega_a\boldsymbol{\nabla}\cdot\Big[\Big(\nu+\frac{\nu_t}{\sigma_\omega}\Big)\boldsymbol{\nabla}\gamma\Big] + 2\beta\omega\gamma\omega_a + \omega_a\frac{\sigma_d}{\omega^2}\gamma\boldsymbol{\nabla}k\cdot\boldsymbol{\nabla}\omega + \\ - \omega_a\frac{\sigma_d}{\omega}\boldsymbol{\nabla}k\cdot\boldsymbol{\nabla}\gamma + \frac{\nu_a(\nu_t-\nu_{max})-\gamma_{2a}}{\omega^2}k\gamma\Big\}d\Omega = 0, \qquad \forall\gamma\in H^1_{\Gamma_i,\Gamma_w}(\Omega) \tag{27}$$

The natural boundary conditions for the optimality system in strong form can be obtained by setting to zero the surface integrals that contain unknown terms or non-integrable functions. The boundary conditions of the adjoint variables for a near wall approach are reported in Table 2. Finally, we present the algebraic equation for the adjoint eddy viscosity and the control equation for the distributed force

$$\nu_a = \frac{k_a}{2}\mathbf{S}(\mathbf{u}):\mathbf{S}(\mathbf{u}) - \mathbf{S}(\mathbf{u}):\boldsymbol{\nabla}\mathbf{u}_a - \frac{1}{\sigma_k}\boldsymbol{\nabla}k\cdot\boldsymbol{\nabla}k_a - \frac{1}{\sigma_\omega}\boldsymbol{\nabla}\omega\cdot\boldsymbol{\nabla}\omega_a \tag{28}$$

$$\mathbf{f} = \frac{\mathbf{u}_a}{\lambda}\ . \tag{29}$$

The force $\mathbf{f}$ on the domain is equal to the adjoint velocity $\mathbf{u}_a$ scaled by the regularization parameter λ. In the case one might be interested in a finite volume discretization it is necessary

Variable	Γ_i	Γ_w	Γ_o
$\mathbf{u}_a\cdot\hat{\mathbf{n}}$	0	0	$\boldsymbol{\tau_a}\cdot\hat{\mathbf{n}} = -\mathbf{u}_a(\mathbf{u}\cdot\hat{\mathbf{n}})$
$\mathbf{u}_a\cdot\hat{\mathbf{t}}$	0	$\boldsymbol{\tau_a}\cdot\hat{\mathbf{n}} = \frac{\nu\mathbf{u}_a\cdot\hat{\mathbf{t}}}{y_d} + \frac{k_a\nu\mathbf{u}\cdot\hat{\mathbf{t}}}{y_d}$	0
p_a	–	–	0
k_a	0	$\boldsymbol{\nabla}k_a\cdot\hat{\mathbf{n}} = \frac{2(k_a+\sigma_d\omega_a)}{y_d}$	$\boldsymbol{\nabla}k_a\cdot\hat{\mathbf{n}} = 0$
ω_a	0	0	$(\nu+\frac{\nu_t}{\sigma_\omega})\boldsymbol{\nabla}\omega_a\cdot\hat{\mathbf{n}} = -(\mathbf{u}\cdot\hat{\mathbf{n}})\omega_a$

Table 2. Adjoint variables boundary conditions with near wall approach.

to recover the strong form of the adjoint system. We integrate by parts (24-27) and obtain the following adjoint system, which is completed by the boundary condition reported in Table 2

$$\boldsymbol{\nabla}\cdot\mathbf{u}_a = 0\ , \tag{30}$$

$$-(\boldsymbol{\nabla}\mathbf{u})^T + (\mathbf{u}\cdot\boldsymbol{\nabla})\mathbf{u}_a + \boldsymbol{\nabla}\cdot[(\nu+\nu_t)\mathbf{S}(\mathbf{u}_a)] + \boldsymbol{\nabla}p_a = a(\mathbf{u}-\mathbf{u}_d) + k_a\boldsymbol{\nabla}k + \\ + \omega_a\boldsymbol{\nabla}\omega + 2\boldsymbol{\nabla}\cdot[(k_a\nu_t+\alpha\omega_a)\mathbf{S}(\mathbf{u})]\ , \tag{31}$$

$$(\mathbf{u}\cdot\boldsymbol{\nabla})k_a + \boldsymbol{\nabla}\cdot\left[\left(\nu+\frac{\nu_t}{\sigma_k}\right)\boldsymbol{\nabla}k_a\right] - k_a\beta^*\omega = b(k-k_d) + \\ + \boldsymbol{\nabla}\cdot\left(\sigma_d\frac{\omega_a}{\omega}\boldsymbol{\nabla}\omega\right) + \frac{\gamma_{2a}-\nu_a(\nu_t-\nu_{max})}{\omega}\ , \tag{32}$$

$$\mathbf{u}\cdot\boldsymbol{\nabla}\omega_a+\boldsymbol{\nabla}\cdot\left[\left(\nu+\frac{\nu_t}{\sigma_\omega}\right)\boldsymbol{\nabla}\omega_a\right]-k_a\beta^*k-2\beta\omega\omega_a=\boldsymbol{\nabla}\cdot\left(\sigma_d\frac{\omega_a}{\omega}\boldsymbol{\nabla}k\right)+ \\ +\frac{\omega_a\sigma_d}{\omega}\boldsymbol{\nabla}k\cdot\boldsymbol{\nabla}\omega+\omega_a\frac{\sigma_d}{\omega^2}\boldsymbol{\nabla}k\cdot\boldsymbol{\nabla}\omega-\frac{\nu_a(\nu_t-\nu_{max})-\gamma_{2a}}{\omega^2}k\ . \tag{33}$$

2.4. Steepest descent algorithm

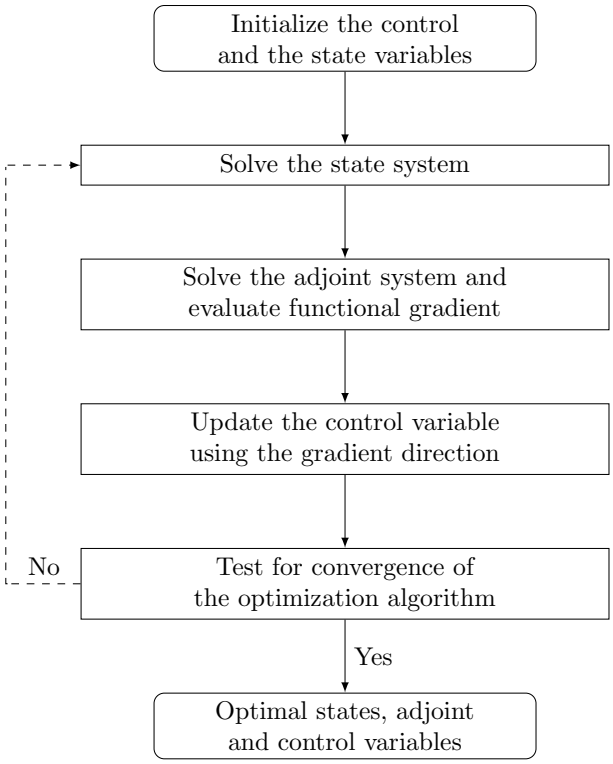

Figure 1. Schematic diagram of the use of steepest descent algorithm.

The system (24-29) is strongly non-linear so it is not possible to solve it with one-shot techniques. We then apply the steepest descent method that is a first-order iterative algorithm for finding the minimum of a functional. A schematic diagram of the general iterative process is shown in Figure 1. Once initialized the state and control variables, the adjoint system is iteratively solved. The adjoint variables are used to update the control parameter that acts on the state variables, until a functional local minimum is reached. The algorithm implemented in our in-house code is presented below.

1) Initialization:
   a) Set up an initial state $(\mathbf{u}^0, p^0, k^0, \omega^0, \nu_t^0)$ solution of the state system;
   b) Set up $\mathbf{f}^0 = 0, r^0 = 1$;
   c) Compute functional $\mathcal{J}^0(\mathbf{u}^0, k^0, \mathbf{f}^0)$;
2) External loop (i index):
   a) Solve the adjoint system and find adjoint variables $(\mathbf{u}_a^i, p_a^i, k_a^i, \omega_a^i, \nu_a^i)$;
3) Internal loop (j index):
   a) Compute control parameter $\mathbf{f}^i = \mathbf{f}^{i-1} + r^{i,j}\left(\mathbf{f}^{i-1} - \mathbf{u}_a^i/\lambda\right)$;
   b) Solve the state system $(\mathbf{u}^{i,j}, p^{i,j}, k^{i,j}, \omega^{i,j}, \nu_t^{i,j})$;

c) Compute functional $\mathcal{J}^{i,j}(\mathbf{u}^{i,j}, k^{i,j}, \mathbf{f}^i)$
- if $\mathcal{J}^{i,j} - \mathcal{J}^{i,j-1} > 0$ set $r_{i,j+1} = 0.7 r_{i,j}$ and return to step (3a);
- if $\mathcal{J}^{i,j} - \mathcal{J}^{i,j-1} < 0$ set $r_{i,j+1} = r^0$ and return to step (2a);
- if $||\mathcal{J}^{i,j} - \mathcal{J}^{i,j-1}||/\mathcal{J}^{i,j-1} < toll$ convergence is reached.

3. Numerical results

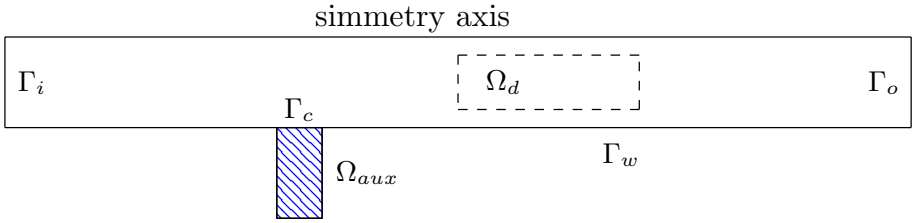

Figure 2. Plane channel geometry. Ω_{aux} is the lifting function auxiliary domain and Ω_d is the target region.

In this section we report some results obtained from the numerical solution of the optimality system described in the previous section. We use a segregated solver for the state and adjoint system and the steepest descent algorithm for the optimal control iterative solution. We use a finite element discretization of the optimality system written in weak form, replacing the infinite dimensional spaces by appropriate finite dimensional spaces. We use a *differentiate-then-discretize* approach since we apply the finite element approximation after computing the Fréchet differentials. We use quadratic finite elements for all variables except the pressure, for which we use linear finite elements to satisfy the *BBL inf-sup* condition needed for the stability of the discrete Navier-Stokes approximation. By doing so we obtain $\mathbf{u}_h$,$\mathbf{u}_{ah} \in \mathbf{X}_h^2(\Omega) \subset \mathbf{H}^1(\Omega)$, p_h,$p_{ah} \in S_h(\Omega) \subset L_0^2(\Omega)$, k_h,k_{ah},ω_h,$\omega_{ah} \in X_h^2(\Omega) \subset H^1(\Omega)$. The algorithm has been implemented in the in-house finite element C++ code FEMuS (available at [14]) which is parallelized with MPI libraries and uses PETSc to handle the algebraic solver of the systems.

We study the two-dimensional geometry shown in Figure 2. The half-channel width W is $0.1m$ and the length L is $1m$. The x-axis is set along the flow direction while the transverse one is y-axis. On the left boundary Γ_i we set an inlet Dirichlet condition $\mathbf{u} = (0.4, 0)\frac{m}{s}$. On the right surface Γ_o a standard outflow boundary condition is imposed. On the symmetry axis a homogeneous Neumann boundary condition is set for all the state and adjoint variables apart from u_y and u_{ay} that vanish on the symmetry axis. On the wall Γ_w we use the near-wall boundary conditions defined in Tables 1 and 2. Let $\Omega_{aux} = [0.3, 0.35] \times [-0.1, 0]$ be the auxiliary domain where the lifting function and control parameter are defined, while $\Omega_d = [0.5, 0.7] \times [0.02, 0.08]$ is the region where the aim to minimize the objective functional. The control surface is denoted with Γ_c. The kinematic viscosity is $\nu = 10^{-5}\frac{m^2}{s}$, so the Reynolds number $Re = UW/\nu$ is 8000 at the inlet of the channel.

3.1. Velocity matching case

In the velocity matching case we set $\mathbf{u}_d = (0.7, 0)\frac{m}{s}$ and solve the optimal control problem with $\lambda = 0.5$, 0.05 and 0.005. On the left of Figure 3 the x-velocity profile on a vertical line at $x = 0.6$ is reported for different values of the regularization λ. The dashed line shows the velocity target $u_{xd} = 0.7$. As λ decreases velocity profiles become more flat with a higher gradient at the wall. On the right of the same Figure the square difference $||u - u_d||^2$ on a vertical line at $x = 0.6$ is shown for $y \in (0.02, 0.08)$. The area under the curve represents $||u - u_d||^2_{L^2}$, i.e. the distance in

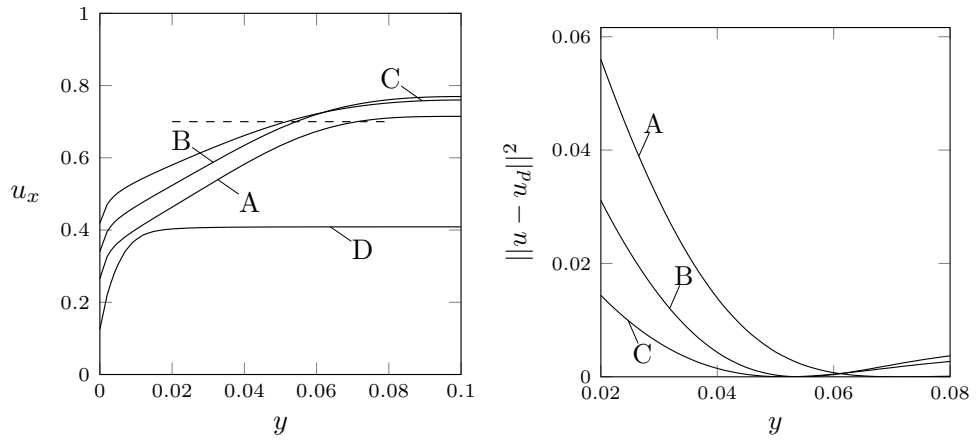

Figure 3. On the left axial velocity u_x, profile on a line at $x = 0.6$. On the right square difference $||u - u_d||^2$ for $y \in (0.02, 0.08)$ on the same line. Result (A) obtained with $\lambda = 0.5$, (B) with $\lambda = 0.05$ and (C) with $\lambda = 0.005$, (D) with no control. The dashed line is the target velocity $u_{xd} = 0.7$.

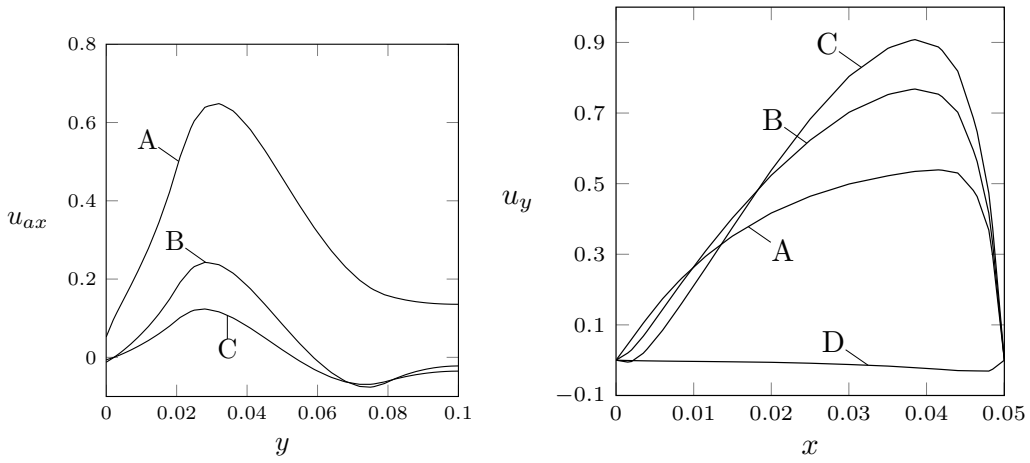

Figure 4. On the left adjoint axial velocity profile u_{ax}, profile on a line at $x = 0.6$. On the right transversal velocity u_y profile on a line at $y = 0$. Result (A) obtained with $\lambda = 0.5$, (B) with $\lambda = 0.05$, (C) with $\lambda = 0.005$ and (D) with no control.

L^2. As it is possible to observe that as λ decreases the L^2-distance from the objective becomes smaller.

In the left of Figure 4 the profile of the adjoint velocity u_{ax} is reported for three values of λ on a vertical line at $x = 0.6$. The adjoint velocity is negative where the fluid velocity has to decrease while shows a strong peak where the velocity has to increase significantly. When λ is smaller the control can act stronger, the velocity is closer to the desired profile and then the adjoint velocity profile is more flat. In the right of the same Figure the lifting function u_y profile on the control boundary Γ_c is reported for different λ values. As λ decreases, the velocity profile is more irregular and harder to be reproduced in the practice. Nevertheless, lower λ values provide a better matching with the desired profile. Finally, in Table 3, the objective functional is reported for the different regularization parameters.

λ	∞	0.5	0.05	0.005
$\mathcal{J}(\mathbf{u}) \cdot 10^5$	53.5874	7.68298	3.79369	1.8032

Table 3. Objective functionals computed with no control ($\lambda = \infty$) and different λ values in the velocity matching profile problem.

3.2. Turbulence enhancement case

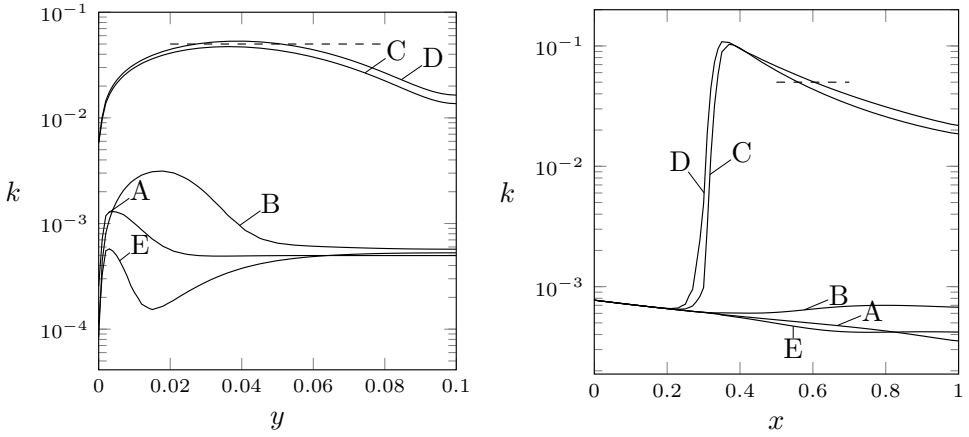

Figure 5. On the left turbulent kinetic energy k profile on a line at $x = 0.6$. On the right on a line at $y = 0.05$. Result (A) obtained with $\lambda = 0.01$, (B) with $\lambda = 0.001$, (C) with $\lambda = 0.0001$, (D) with $\lambda = 0.00001$, (E) with no control. The dashed line is the target value $k_d = 0.05$.

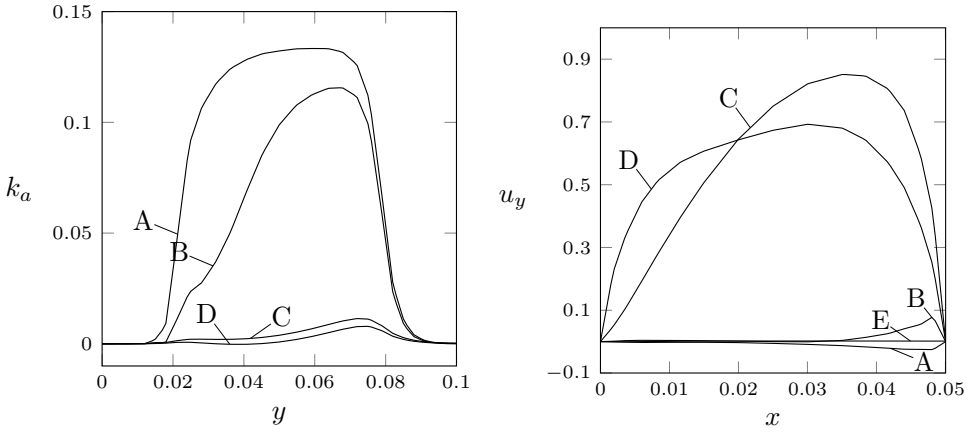

Figure 6. On the left adjoint turbulent kinetic energy k_a profile on a line at $x = 0.6$. On the right transversal velocity profile on a line at $y = 0$. Result (A) obtained with $\lambda = 0.01$, (B) with $\lambda = 0.001$, (C) with $\lambda = 0.0001$, (D) with $\lambda = 0.00001$, (E) with no control.

In this section we consider a turbulence enhancement problem which consists in increasing the turbulent kinetic energy k. We set $a = 0$, $b = 1$ and the target kinetic energy value $k_d = 0.05$, two orders of magnitude higher than that of the not controlled case. We solve the optimal control problem with $\lambda = 0.01$, 0.001, 0.0001 and 0.00001.

On the left of Figure 5 the turbulent kinetic energy k profiles on a line crossing the controlled region Ω_d at $x = 0.6$ are reported for different amount of regularization (A-D) and for the not controlled case (E) for comparison. We notice that by reducing λ the peak of the turbulent kinetic energy k grows and moves towards the center of the channel, where the objective functional is computed. On the right of the same Figure are reported k profiles on a line aligned with the main fluid flow at $y = 0.05$. Upstream of the auxiliary domain Ω_{aux} the flow regime is not altered by the control, while downstream, $x > 0.3$, the desired turbulence enhancement is obtained for cases C-D. The adjoint turbulent kinetic energy k_a profile is reported on a line at $x = 0.6$ on the left of Figure 6. When considering higher λ values we obtain that k is generally far from k_d then the source term $k - k_d$ in the k_a-equation is sizeable thus leading to adjoint turbulence peaks. The lifting function u_y profile over the control boundary Γ_c is reported for different λ values on the right of the same Figure. In order to enhance the turbulence in the middle of the channel more fluid has to be injected through the control boundary, with higher values of λ the control is too weak, while choosing $\lambda \leq 0.0001$ the optimal injection velocity profile is found. Finally, the objective functionals are reported in Table 4.

λ	∞	0.01	0.001	0.0001	0.00001
$\mathcal{J}(\mathbf{k}) \cdot 10^6$	15.4392	15.3898	15.0848	1.42287	1.07756

Table 4. Objective functionals computed with no control ($\lambda = \infty$) and different λ values in the velocity matching profile problem.

4. Conclusions

In this work we have studied a boundary optimal control problem for the Reynolds Averaged Navier-Stokes system coupled with a two-equation turbulence model in Wilcox $k-\omega$ formulation. We have used a *lifting function* approach that allows to reformulate a boundary control problem into a distributed one. In addition, the control parameter obtained belongs to its natural space. The distributed parameter is a force acting on an auxiliary domain that shares with the domain the boundary where the optimal boundary control is searched. Moreover, the force profile obtained can be used to design flow injection section. The optimality system has been derived with the minimization of the Lagrangian. We have used different objective functionals to study a velocity matching or a turbulence enhancement problem. We have obtained the adjoint equations and adjoint boundary conditions. The numerical simulations presented have shown the effectiveness of this approach in achieving the desired minimization and robustness.

References

[1] Gunzburger M D, Hou L and Svobodny T P 1992 *SIAM journal on control and optimization* **30** 167–181
[2] Gunzburger M and Manservisi S 2000 *SIAM J. Control Optim* **39**(2) 594–634
[3] Wilcox D 1994 *Turbulence Modeling for CFD* (DCW Industries, Incorporated)
[4] Bewley T R, Moin P and Temam R 2001 *Journal of Fluid Mechanics* **447** 179–225
[5] Manservisi S and Menghini F 2016 *Computers & Fluids* **125** 130–143
[6] Gunzburger M and Manservisi S 2000 *Comput Methods Appl Mech Eng* **189**(3) 803–823
[7] Bornia G 2013 *AIP Conference Proceedings* vol 1558 (AIP) pp 879–882
[8] Aulisa E, Bornia G and Manservisi S 2015 *Commun. Comput. Phys.* **189**(3) 621–649
[9] Gunzburger M D 2003 *Perspectives in flow control and optimization* vol 5 (Siam)
[10] Brenner S and Scott R 2007 *The mathematical theory of finite element methods* vol 15 (Springer Science)
[11] Bredberg J 2000 *Chalmers University of Technology, Internal Report 00/4. Goteborg*
[12] Bornia G, Gunzburger M and Manservisi S 2013 *Commun. Comput. Phys.* **14** 722–752
[13] Manservisi S and Menghini F 2016 *Computers & Mathematics with Applications* **71** 2389–2406
[14] Code FEMuS URL `https://github.com/FemusPlatform/femus`